Transactions of the Materials Research Society of Japan 29[4] 1647-1650 (2004)

Structural Characterization of Oriented L1o-FePd Nanoparticles

K. Sato and Y. Hirotsu
The Institute of Scientific and Industrial Research, Osaka University
8-1 Mihogaoka, Ibaraki, 567-0047 Osaka, Japan
e-mail: sato@sanken.osaka-u.ac.jp

Nanostructure of 10-nm-sized L1o-FePd nanoparticles has been characterized by transmission electron microscopy. Particle size distribution followed a log-normal type distribution function and they did not practically change on annealing up to 873K, which can be attributed to an well-isolation of particles and an "anchoring effect" of Pd seed nanoparticles. EDS analysis using a nano-probe indicated a composition difference from particle to particle, but the distribution is narrow with a standard deviation of only 3at.%Pd. Post-deposition annealing at the temperatures higher than 723K lead to a formation of the L1o ordered phase. Long-range order parameter was determined by electron diffraction by exciting the *hh0* systematic reflections. The obtained order parameters were 0.65 ± 0.02 and 0.79 ± 0.02 for the specimen after annealing at 873K for 1 and 10h, respectively. Electron energy-loss spectroscopy revealed that no obvious oxidization occurred in the present specimen. Coercivity at 10K was about as twice as that of 300K, indicating the existence of thermal effect. The largest coercivity obtained was 3.5kOe at 300K after annealing at 873K for 1h. Considering the determined LRO parameters, we can expect that the larger coercivity will be obtained by heat treatment under the longer annealing at 873K or higher temperature annealing.
Key words: FePd, Nanoparticles, LRO parameter, Nanobeam, EDS, EELS

1. INTRODUCTION

Recent development of high-density magnetic storage media results in a rapid increase of the recording density, which almost reached a maximum value for the presently used longitudinal continuous media [1]. For future ultra-high density recording media, isolated nanoparticle assembly of L1o ordered alloy is attracting much interest in these years. The current problems to be solved are low temperature synthesis of the L1o phase, periodic arrangement of particles with finite sizes, and orientation control of the magnetic easy axis (c-axis of the L1o structure). Besides these points, it is necessary to reveal a relation between long-range order (LRO) parameter and hard magnetic properties of L1o nanoparticles from the scientific viewpoints.

Equiatomic FePd alloy is well known as a hard magnet due to its high magnetocrystalline anisotropy energy originated from the L1o ordered structure. Because of these characteristics, L1o-FePd nanoparticle is expected as one of the candidates for future ultra-high density magnetic storage media, while there is a few article concerning its precise structural characterization [2, 3]. The authors have investigated the nanostructure and magnetic properties of oriented FePd nanoparticles with 2 dimensional dispersion [2, 3].

In this paper, results of the atomic ordering process and the LRO parameter for 10-nm-sized FePd nanoparticles studied by transmission electron microscopy (TEM) are presented and their relations to hard magnetic properties are briefly discussed.

2. EXPERIMENTAL

Specimen preparation was performed by a successive deposition of Fe and Pd onto the single crystalline NaCl substrate cleaved in air using an electron-beam deposition apparatus. In the fabrication process, we took advantage of the epitaxial growth of Fe onto Pd "seed" nanoparticles, which were epitaxially grown on the NaCl surface. Substrate temperature was kept at 673K during the deposition. After the deposition of Fe and Pd, we further deposited Al_2O_3 as a cover layer in order to protect particles from oxidization. Precise fabrication procedure is referred to in our previous articles [2]. Structural characterization was performed by TEM (JEM-2010 and –3000F with PEELS and EDS). EDS analysis showed that the mean composition of the fabricated specimen was in the range between 49 and 60 at.%Pd. Heat treatment for promoting the atomic ordering was performed using a high-vacuum furnace. In-situ annealing in TEM was also performed by using a specimen heating stage. Heating and cooling rates were about 5 and 10K/min, respectively. Magnetic properties were measured using a SQUID magnetometer (Quantum Design, MPMS-5S).

3. RESULTS AND DISCUSSION

The fabricated specimen was composed of bcc-Fe and Pd nano-complex particles with mutual fixed orientation as follows: $[100]_{Fe} \parallel [100]_{Pd}$, $(011)_{Fe} \parallel (010)_{Pd}$ [2]. In-situ annealing in TEM after the deposition revealed that the atomic ordering reaction started at temperatures above 723K, which was known by the appearance of 110 superlattice reflections in the selected area electron diffraction (SAED) pattern. Figure 1 shows a series of SAED patterns under the elevated annealing temperatures. The mean composition was Fe-58at.%Pd. In Fig.1(c), reflections from bcc-Fe are seen besides the 110 superlattice reflection from the L1o structure, indicating that both of the alloying and the atomic ordering reactions proceed almost simultaneously on the

post-deposition annealing. At temperatures above 773K, intensities of superlattice reflections became strong and 001 reflections appeared in addition to 110 as shown in Figs.1(d) to 1(f), suggesting a proceeding of the L1o ordering. This feature coincides well with the increase of magnetic coercivity above 773K [2]. In Fig.1(f), though the intensity of 110 reflection is strong, weak reflections from residual Fe still remained (indicated by single arrow heads in Fig.1(f)). Because of the in-situ annealing with a finite heating rate, the keeping time at each temperature is not sufficient for promote the alloying reaction. Actually, in the case of ex-situ annealing with a keeping time of 1h, it was already confirmed that reflections from the residual Fe disappear at 823K [3]. The annealing temperature of 723K corresponds to $0.35T_m$ where T_m means the melting temperature of the equiatomic Fe-Pd alloy. Such a high temperature annealing condition necessary for ordering indicates that the proceeding of the L1o ordering reaction must be the volume diffusion via vacancy mechanism even in 10-nm-sized particles.

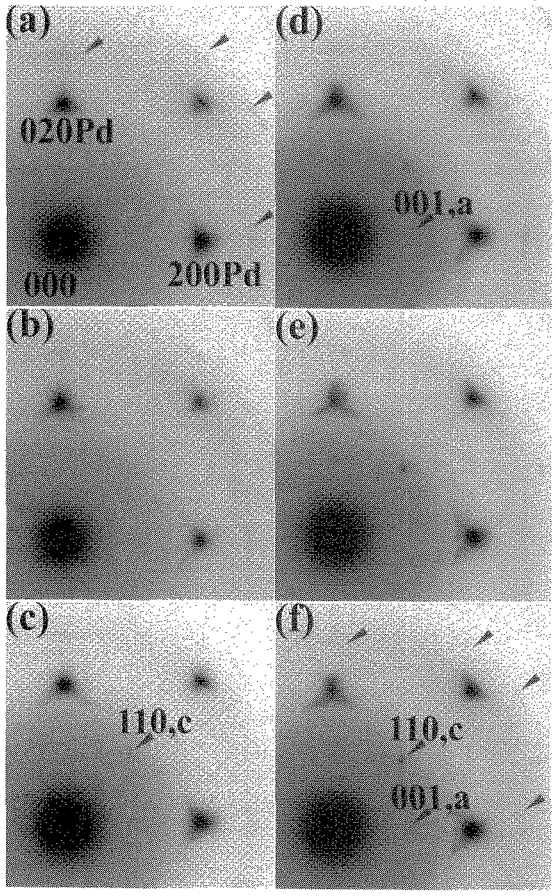

Fig.1. A series of SAED patterns observed by in-situ annealing in TEM at the temperatures between 300 and 873K. (a)as-deposited., (b)673K, (c)723K, (d)773K, (e)823K, (f)873K. The heating rate was 5K/min. In Fig.1(a), single arrow heads indicate 200 and 211 reflections from bcc-Fe (see Ref. 6). Indices 110,c and 001,a indicate the superlattice reflections from the L1o-FePd nanoparticles with c-axis oriented normal and parallel to the film plane, respectively.

Table I Mean particle size and deviation for FePd nanoparticles with different annealing conditions.

	As-depo.	873K-1h	873K-10h
D / nm	11.3	11.1	11.3
lnσ	0.23	0.18	0.21

Particle size distribution was almost conserved during the annealing at the temperatures up to 873K since the mean size and deviation did not practically change on annealing, which can be attributed to an well-isolation of particles and an "anchoring effect" of Pd seed nanoparticles (see Table I). Particle size distribution followed a log-normal type distribution function. Figure 2 shows the TEM image and the corresponding SAED pattern for FePd nanoparticles after annealing at 873K for 10h. A quite homogeneous distribution of nanoparticles in a wide area is achieved in our fabrication technique. It is noted that no obvious oxidization occurred in the present specimen during the annealing. The white line ratio (intensity ratio of L_3 and L_2 edges) of Fe in FePd nanoparticles obtained by electron energy-loss spectroscopy (EELS) was approximately 3.4, which is close to the value for bcc-Fe [4-6] but smaller than that of iron oxide [4, 7].

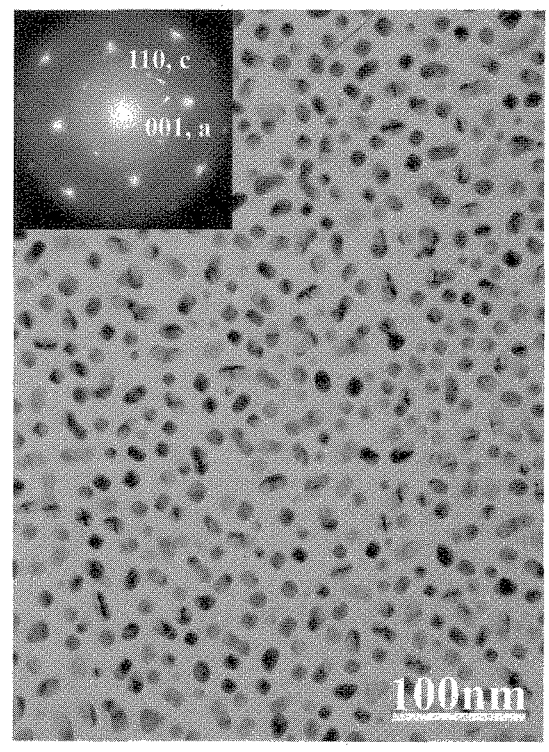

Fig.2. TEM image and corresponding SAED pattern for FePd nanopartilces after annealing at 873K for 10h. No obvious coalescence of particles occurred after the annealing (See Table I).

EDS analysis using a nanometer-sized electron probe revealed that there is a composition difference from particle to particle. Figure 3 shows the histogram of alloy composition of 30 particles analyzed by nano-EDS, which followed a Gaussian type distribution function

with a standard deviation of 3at.%Pd. This result supports the fact that each Pd "seed" particles act as nucleation sites of bcc-Fe particles in the successive deposition process. Narrow distribution of alloy composition is useful for discussing the ordering process of the assembly of FePd nanoparticles, since order-disorder transformation temperature of Fe-Pd alloy strongly depends on the alloy composition as shown in the equilibrium phase diagram [8].

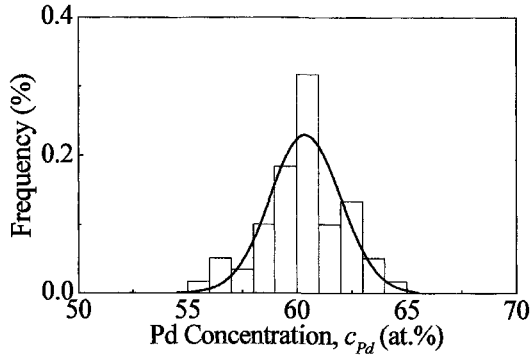

Fig.3. Alloy composition distribution measured by nanobeam EDS analysis. The probe size corresponded to each particle size. The mean composition was 60at.%Pd with standard deviation of 3at.%Pd. EDS analysis from a wide area showed a same mean composition.

The LRO parameters for 10-nm-sized FePd nanoparticles prepared under different conditions were determined by electron diffraction. Since the scattering power of atoms for electrons is about 10^4times larger than that for x-rays, electron diffraction has a great advantage for obtaining weak superlattice reflections from very small particles. In the determination process, *hh0* systematic reflections were excited by tilting the specimen film, which reduces the diffracted beams and can largely simplify the multiple scattering events among the transmitted and the diffracted waves [9]. Intensity ratio, I_{110} / I_{220} was measured from the SAED pattern with *hh0* systematic reflections. Specimen thickness was estimated to be 8 ± 2nm by electron holography. Based on the multi-slice calculations, we determined the LRO parameters using the intensity ratio measured by electron diffraction. Precise determination process and the effect of several experimental conditions will be published in elsewhere [10]. The LRO parameters of 0.65 ± 0.02 and 0.79 ± 0.02 were obtained for the specimen (Fe-58at.%Pd) after annealing at 873K for 1 and 10h, respectively, assuming the temperature factors of bulk Fe and Pd [11].

In Fig.4, a calculated relation between the intensity ratio and the LRO parameter for the Fe-58at.%Pd alloy is drawn by a solid line. Broken lines indicate the experimentally obtained intensity ratios. Considering the alloy composition of 58at.%Pd, the maximum LRO parameter to be realized is at most 0.84 for this alloy. So it is noted that annealing for 10h at 873K lead to a formation of almost fully ordered FePd nanoparticles.

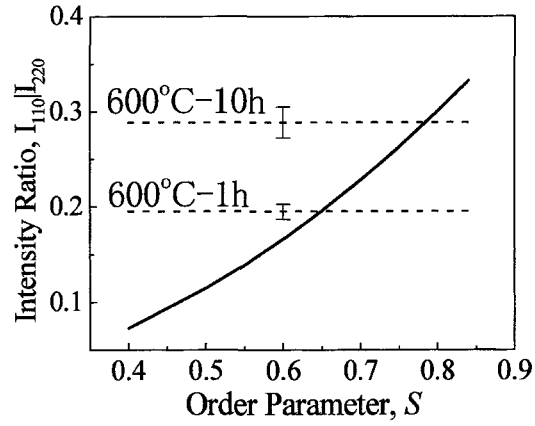

Fig.4. LRO parameter dependence of the intensity ratio, I_{110}/I_{220} obtained by the multi-slice simulations. Broken lines indicate the experimentally obtained intensity ratios under the accelerating voltage of 300kV.

Magnetic hysteresis loops for Fe-58at.%Pd nanoparticles after annealing at 873K for 1h were measured at 300K with the external field both perpendicular and parallel to the film plane along the principal axes of the NaCl substrates. The obtained results are shown in Fig.5(a) and 5(b). The obtained maximum coericvity was 3.5kOe, while a larger coercivity of 10kOe at 300K and 20kOe at 10K are expected for 10-nm-sized L1o-FePd nanoparticles assuming the random orientation of c-axes [12]. Since the LRO parameter for this specimen was 0.65 as shown in Fig.4, it is expected that the larger coercivity will be obtained by heat treatment under the longer annealing at 873K or higher temperature annealing, if we could safely form a fully ordered nanoparticles without any particle coalescence on annealing.

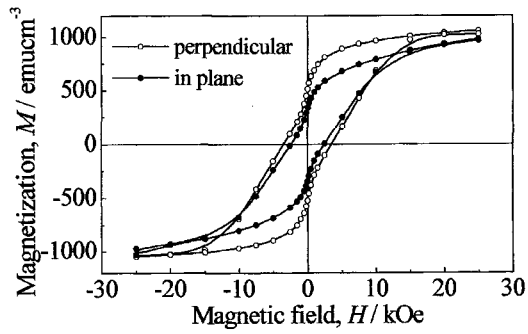

Fig.5 Magnetic hysteresis loops for Fe-58at.%Pd nanoparticles after annealing at 873K for 1h. Open and solid circles represent the results with external field of perpendicular and parallel to the film plane. Here, shearing correction was not performed for the perpendicular magnetization curve.

Magnetic hysteresis loops of FePd nanoparticles after annealing at 823K for 1h were measured in the temperature range between 10 and 300K. Mean particle size was 11nm with alloy composition of 49at.%Pd. Magnetic field was applied parallel to the film plane in the measurements. Hysteresis loops measured at 10 and 300K are shown in Fig.6. The obtained results indicated

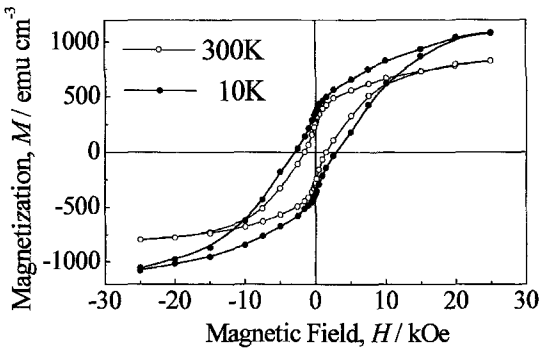

Fig.6. In-plane magnetization curves for Fe-49at.%Pd nanoparticles after annealing at 823K for 1h. Open and solid circles represent the results measured at 300 and 10K, respectively. Increase of coercivity at 10K indicates the existence of thermal fluctuation of magnetization at 300K.

that saturation magnetization and coercivity increased with decreasing the temperature, while the remanence remained at a constant value of about 0.35 in the whole temperature range. These are listed in Table II. It is interesting that the coercivity at 10K is about as twice as that of 300K, indicating the existence of thermal fluctuation of magentization for the present 10-nm-sized L1o-FePd nanoparticles.

Table II Coercivity (H_c), Saturation magnetization (M_s) and normalized remanence for Fe-49at.%Pd nanoparticles after annealing at 823K for 1h. Magnetization was obtained by using the mean deposited thickness of FePd monitored by a quartz oscillator during the deposition. Here, M_s is defined as the magnetization at 25kOe. These are extracted from the measured hysteresis loops at each temperature.

	300K	200K	100K	10K
H_c /kOe	1.5	2	2.5	2.9
M_s /emucm^{-3}	813	866	923	1074
M_r / M_s	0.34	0.36	0.37	0.35

4. CONCLUSION

Nanostructure of 10-nm-sized L1o-FePd nanoparticles has been characterized by transmission electron microscopy. Post-deposition annealing at the temperatures higher than 723K ($0.35T_m$) lead to a formation of the L1o ordered phase. Such a high temperature annealing condition necessary for ordering indicates that the proceeding of the L1o ordering reaction must be the volume diffusion via vacancy mechanism even in 10-nm-sized particles. Particle size distributions did not practically change on annealing up to 873K due to the "anchoring effect" of Pd seed nanoparticles, indicating the fact that both the alloying and the ordering reactions proceed within each isolated nanoparticles. EDS analysis using a nano-probe indicated a composition difference from particle to particle, but its distribution was narrow with a standard deviation of only 3at.%Pd. Long-range order parameter was determined by electron diffraction by exciting the *hh0* systematic reflections. The obtained order parameters were 0.65 ± 0.02 and 0.79 ± 0.02 for the specimen after annealing at 873K for 1 and 10h, respectively. EELS analysis revealed that no obvious oxidization occurred in the present specimen. Coercivity at 10K was about as twice as that of 300K, indicating the existence of thermal fluctuation of magentization. The largest coercivity obtained was 3.5kOe after annealing at 873K for 1h. Considering the presently analyzed structural characteristics, it is expected that the larger coercivity will be obtained by heat treatment under the longer annealing at 873K or higher temperature annealing.

ACKNOWLEDGMENTS

The authors wish to thank Profs. T. Kawai and H. Tanaka of ISIR, Osaka University for supporting the SQUID measurements, Dr. T Hirayama of JFCC for electron holography observations, and Dr. T. Hanada of ISIR for valuable discussions on EELS. This study was supported by the Center of Excellence (COE) Program at ISIR-SANKEN, Osaka University, Grant-in-Aid for Scientific Research (Nos. 14205094, 13555189 and 13750612) and Special Coordination Funds for Promoting Science and Technology on "Nanohetero metallic materials" from the Ministry of Education, Culture, Sports, Science and Technology. This study was partly supported by Research Foundation For Materials Science.

REFERENCES

[1] D. Weller and M. F. Doerner, *Annu. Rev. Mater. Sci.*, **30**, 611-644 (2000).
[2] K. Sato, B. Bian and Y. Hirotsu, *Jpn. J. Appl. Phys.*, Part2 **39**, L1121-L1123 (2000).
[3] K. Sato and Y. Hirotsu, *J. Appl. Phys.*, **93**, 6291-6298 (2003).
[4] R. D. Leapman, L. A. Grunes and P. L. Fejes, *Phys. Rev.*, B **26**, 614-635 (1982).
[5] N. Tanaka, F. Yoshizaki and K. Mihama, *Mater. Sci. Eng.*, **A217/218**, 311-318 (1996).
[6] B. Bian and Y. Hirotsu, *Jpn. J. Appl. Phys.*, Part2 **36**, L1232-L1235 (1997).
[7] C. Colliex, T. Manoubi and C. Ortiz, *Phys. Rev.*, B **44**, 11402-11411 (1991).
[8] "Binary Alloy Phase Diagrams", 2nd ed., Ed. by T. B. Massalski, H. Okamoto, P. R. Subramanian and L. Kacprzak, ASM International, Materials Park, Ohio (1990) p.1751.
[9] K. Sato and Y. Hirotsu, *Mater. Trans.*, **44**, 1518-1522 (2003).
[10] K. Sato et al. in preparation.
[11] N. M. Butt and J. Bashir: *Acta Cryst.*, **A44**, 396-398 (1988).
[12] H. Pfeiffer, *Phys. Stat. Sol.*, **A118**, 295-306 (1990).

(Received October 8, 2003; Accepted February 9, 2004)